A Review of Frequency Response Solution for Type - 3 Wind Turbines Using Energy Storage Device

Atiqul Islam*‡, Sandeep Nimmagadda*, Anitha Subburaj*, Stephen. B. Bayne*

*Department of Electrical & Computer Engineering, Texas Tech University, Lubbock, Texas-79409, USA

(atiqulwindenergy@outlook.com, sandeep.windenergy@gmail.com, anitha.subburaj@ttu.edu, stephen.bayne@ttu.edu)

‡ Corresponding Author: Atiqul Islam, Texas Tech University, Lubbock, Texas-79409, USA, Tel: +01 806 786 3968, Fax: +01 806 742 1281, atiqulwindenergy@outlook.com

Received: 30.06.2016 Accepted: 06.08.2016

Abstract - This paper identifies the current approaches to provide the frequency response from type 3 (Doubly Fed Induction Generator based) wind turbines to support the grid during power imbalance. It discusses the use of energy storage devices for providing support during frequency deviation. The paper mainly focuses on the approach to connect the energy storage with the wind turbine through the DC coupling capacitor and use the already available wind turbine AC/DC/AC converter for power conversion. The process to choose an energy storage device and appropriately sizing it for desired support is stated. It also discusses the wind turbine controller strategy modification to properly operate the energy storage device and provide required support. Finally, the study shows simulation results indicating the validation of connecting energy storage through DC coupling capacitor and the updated control algorithm method in different operating condition.

Keywords DFIG wind turbine, frequency response, power imbalance, energy storage, DC capacitor, converter controller.

1. Introduction

Improvements in the renewable-energy technology and policy changes are forcing increased amount of wind energy in the US grid [1]. Wind energy is ensuring a cleaner environment by providing green energy, but it is also posing some serious technical challenge to the grid operators. Providing frequency response from wind turbines during grid power imbalance is one of the major concerns. Interconnection operators at different regions in USA carried out studies to identify the frequency response and noticed a decline in the response [2]. Western interconnection is reporting a decline of 20MW/0.1 Hz/Year in the span of 5 years (1998-2002). Similarly Eastern interconnection region is also reporting a decline of 70 MW/0.1 Hz/year in the span of 8 years (1994-2002). Actual frequency response estimation in Texas ERCOT region is challenging due to the presence of two sets of interruptible load for handling power imbalance issues. Reports suggest a flat characteristic in the frequency response curve over the years in the span of 7 years [3]. However, actual frequency response in the ERCOT may also be declining. The authorities in the respective areas are blaming the wind-related generation sources for the decline of frequency response. The authorities are also imposing stricter rules for wind energy to comply with the frequency response requirement.

Normally, the wind turbines are not supportive during the power imbalance events. During power imbalance, frequency response from the generating units is provided by either reducing or increasing output power. Conventional synchronous generator can sense the system frequency and increase or decrease the power output. Wind generator can decrease the output power by pitch control, but sudden increase in the output is normally impossible due to the fact that the turbine is completely dependable on the available wind speed. To provide frequency response from wind turbine, some supportive method or control upgrade is necessary. Current available solutions mainly focus on control upgrades to provide the frequency response. Studies revealed that, in the stator flux oriented frame, the system frequency is inversely related to the generator torque when the current is kept constant [4]. However even in that situation, the change in output power is minimal while the

torque is varied. So it fails to serve the purpose of providing a desired frequency response. Literature solutions also indicate that the frequency response of the wind turbine in a DFIG based generator can be improved by using two main methods; a) emulate inertial response from wind turbine by updating control response or b) use the droop characteristics of the wind turbine.

To emulate the inertial response from a wind turbine, the turbine needs to increase its power output for a short period of time. It is achieved by considering the Rate of Change of Frequency (ROCOF) and reducing the wind speed for a brief period of time [4-10]. While the suggested methods can provide frequency response, it has certain risks and performance issues associated. The wind turbine may stall during the stage of providing the inertial support. The danger associated with the sudden stall of wind turbines during frequency deviation can be catastrophic. Stalled wind turbine will reduce the grid generation further and increase the frequency deviation and Rate of Change of Frequency (ROCOF). Increased ROCOF and frequency deviation is likely to trigger the tripping of further generating units, creating a cascading event. These phenomena can lead to a complete blackout [11]. In case the wind turbines do not stall, it creates further issue by extracting extra power from the grid during speed up and thus creates a secondary frequency dip.

In case of the droop control, the wind turbine is operated in a non-optimal operating condition. During the frequency deviation, the turbine is shifted into an optimal operating condition to extract the additional power. The non-optimal condition can be achieved by two different approaches, by increasing the pitch angle value or by operating the wind turbine constantly at a higher speed than the nominal [12-14]. These processes also have some limitations. In the method of pitch control, frequency response is slow. Furthermore the turbine produces reduced output during normal operating condition. As a result, the total operating cost for the wind-turbine increases. In case of over speed, the turbine needs to operate constantly at a speed greater than the nominal speed. So the power propagation through the converter is high due to increased slip. Eventually, the converter size needs to be increased. Also operating at higher speed than nominal increases the wear and tear of the wind turbine and in turn reduces the operating life time.

The main motivation of this paper is to review and verify alternative solutions for frequency response from wind turbines by overcoming the limitations stated in the previous paragraphs. The paper focuses on the solutions to integrate energy storage devices with the turbine to provide the desired frequency response by charging and discharging the battery accordingly. Among different wind turbine configurations, Type 3 or Doubly Fed Induction Generator (DFIG) based wind turbines are considered during this study. The organization of the paper is as followed. Section 2 discusses the impact of energy storage devices with respect to the frequency response. It also briefly discusses the process to choose the proper energy storage device for wind turbines. Section 3 discusses basic configuration of the DFIG based wind turbines, and the converter control methodology. Section 4 states the control algorithm to connect the energy storage device through the DC capacitor. In section 5 simulation and results were discussed. Finally in section 6 the paper ends by stating all the important findings from the study.

2. Frequency Response & Energy Storage Device

Electrical power demand and supply to a power system should be always matched for stable operation. If the supply is less than the demand, the system frequency goes down from the nominal value, similarly when the supply is greater than the demand, the system frequency increases from the nominal value. The actions taken by generation sources to arrest the frequency deviation and bring back the system frequency to its nominal value is described as the frequency response [15]. Frequency response can be categorized into several different types depending on the response time and the nature of support [15]. Inertial response is one of the first steps of the total system frequency response. It acts in the first few seconds of the power imbalance event and try to slow down the frequency deviation.

Researchers have been studying the inertial response from DFIG based wind turbines for several years, and it has been identified that the turbines have a very low or zero inertial response contribution to the grid. The wind turbines basic target is to operate in an optimal condition and extract as much power available from the wind speed. The conditions lead the turbines to operate without any reserve at all. In case when the grid frequency goes over the nominal value, the wind turbine can contribute by increasing the pitch angle and thus reducing the output power. But in case of grid frequency goes lower than the nominal value; the wind turbine can only generate the available power from the wind speed and thus are unable to participate in the frequency response.

The relation between grid inertia, power imbalance and frequency deviation can be described by equation (1)

$$\partial f / \partial t = \Delta P / 2H \quad (1)$$

Here ∂f is the frequency deviation, ΔP is the power imbalance between the generated and the dispatched power and H is the power system inertia [11, 16, 17].

$$H = \frac{1/2 J\omega^2}{MVA} \quad (2)$$

Here, J is the moment of inertia, ω is the speed of rotation and MVA is the MVA rating of the power system [6, 16].

Equation (1) also defines system Rate of Change of Frequency (ROCOF). It is obvious from equation 1 that if the amount of power difference (ΔP) remains same, then frequency deviation will be inversely proportional to system inertia. Similarly if the system inertia (H) remains same then the frequency deviation will be proportional to the power difference between generation and load (ΔP).

Introducing more and more wind power in the system reduces the system inertia and thus increases the chance of

greater frequency deviation. Such a high frequency deviation can in turn increase the chance of more generator tripping and create a huge network disturbance [11].

Instead of providing direct inertial response, wind turbines can create an artificial reserve by operating with energy storage device. Energy storage can supply the extra power during power imbalance. Response during frequency deviation with the energy storage integrated can be described by equation (3).

$$\partial f/\partial t = \frac{P_{windgen} - P_{Load} + P_{energystorage}}{H} \quad (3)$$

Here, $P_{windgen}$ is the power generated by wind turbine, P_{Load} is the demand at the grid and $P_{energystorage}$ is the extra power supplied by energy storage device. It is obvious from equation (3) that as the extra power from energy storage reduces the total power imbalance between load and generation. ROCOF and total frequency deviation will also decrease.

There are different types of energy storage devices, such as Battery Energy Storage, Fly wheel, compressed air, super capacitors, pumped hydro, super magnetic energy storage etc. Not all of the energy storage technologies are suitable to connect with the wind turbines considering the size, cost and energy density. For turbine level support, Battery Energy Storage System (BESS) provides the best solution considering the cost, instant power availability, two way power share capability, round trip efficiency, longer life span and high-energy density [17-19]. Distinct battery technology can be used for BESS development. Some commonly available battery technologies are Lead acid, Li-Ion, Nickel Cadmium, Nickel-Metal Hydride etc. Lead acid topology is one of the oldest battery systems available. But it has limitations, such as, low efficiency and nonexistent cycling capacity. The above-mentioned limitations make Lead-acid batteries unsuitable for developing the wind-turbine application. Nickel- Cadmium batteries are low-cost and long lasting. However the batteries have low energy density and also use toxic material during production. So the Nickel-cadmium batteries are not suggested to produce BESS. Nickel-metal hydride batteries are better solutions by producing batteries with higher-energy density, but it has a major disadvantage of higher self-discharge [20, 21]. Considering all the facts; Li-Ion batteries provide the best option for producing BESS. It has the advantage of low cost, high-energy density and relatively higher efficiency. During this study, Li-Ion batteries are considered for developing the BESS.

3. Basic DFIG Configuration & Converter Control

Figure 1 shows the basic block diagram of the DFIG based wind turbine system. DFIG consists of a wound rotor induction generator. The stator of the generator is directly connected to the power-supply grid, whereas the rotor of the turbine is connected to the grid through a bi- directional power electronic converter. Power ratio of the rotor to the stator is one third. That helps to reduce the size of the power electronic converter. The active and reactive power control set points of the wind turbine comes from the wind farm controller. Wind farm senses the grid conditions and also takes input from the Transmission Service Operators (TSO) to generate proper set points for the active and reactive power [22].

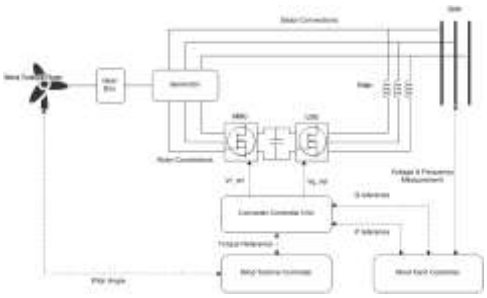

Fig. 1. Basic block diagram of DFIG Wind Turbine

The AC/DC/AC converter in the system helps the wind turbine to properly connect to the grid by synchronizing with grid voltage and frequency. It has two main parts, Machine Side Converter (MSC) and Line Side Converter (LSC). Both of those converters use six Insulated Gate Bipolar Transistor (IGBT) Switches. Control signals of the switches are calculated by comparing three-phase reference voltages with high-frequency triangular waves. Reference voltages for both MSC and LSC are calculated using the vector control algorithm.

The aim of the MSC controller is to follow active and reactive power control set points that have been acquired from the wind farm controller. MSC control is achieved using stator voltage reference frame. Three-phase voltages are converted into D-Q axis frame and required set points are followed using PI controllers. Mathematical expression related with the vector control is given below in equation 4 to 7 [22]

$$I_{Dr_{set}} = \frac{(P_{ref} - P_{lsc})}{V_{sd}} \cdot \frac{L_s}{L_m} - \frac{I_{Qs} R_s}{L_m} \quad (4)$$

$$I_{Qr_{set}} = -\frac{(Q_{ref} - Q_{lsc})}{V_{sd}} \cdot \frac{L_s}{L_m} - \left(\frac{V_{sd}}{L_m} - \frac{I_{Ds} R_s}{L_m}\right) \quad (5)$$

$$V_{Dr} = K_{pmsc} \cdot \left(I_{Dr_{set}} - I_{Dr}\right) + K_{imsc} \int \left(I_{Dr_{set}} - I_{Dr}\right) . dt + s . \left(\frac{L_m}{L_s} . V_{Ds} - \sigma . L_r . I_{Qr}\right) \quad (6)$$

$$V_{Qr} = K_{pmsc} \cdot \left(I_{Qr_{set}} - I_{Qr}\right) + K_{imsc} \int \left(I_{Qr_{set}} - I_{Qr}\right) . dt - s . \sigma . L_r . I_{Dr} \quad (7)$$

Here, $I_{Dr_{set}}$ & $I_{Qr_{set}}$ are the D and Q axis rotor current set point, P_{ref} & Q_{ref} are the active reactive power set point, P_{lsc} & Q_{lsc} are the line side converter power, I_{Ds} & I_{Qs} are the D and Q axis stator current, I_{Dr} & I_{Qr} are the D and Q axis rotor current, V_{Ds} & V_{Qs} are the D and Q axis stator voltage, V_{Dr} & V_{Qr} are the D and Q axis rotor voltage, R_s is the stator resistance, L_s, L_r & L_m are the stator rotor and mutual inductance, s is the slip, $\sigma = 1 - \frac{L_m^2}{L_s L_r}$ and K_{pmsc} & K_{imsc} are the proportional and integral gain of the converter PI controller. Once V_{Dr} and V_{Qr} are calculated, they are converted back into three phase system and compared with

triangular waves to calculate the gate signals for the MSC IGBT switches.

Main aim of the LSC is to regulate the dc link voltage within a certain limit. LSC is also controlled in the stator voltage oriented frame. Governing equations of the LSC has been given below [22]

$$I_{Qg_{set}} = -\frac{Q_{lsc\_ref}}{|V_g|} \quad (8)$$

$$I_{Dg_{set}} = K_{pdc}.\left(V_{DC_{set}} - V_{DC}\right) + K_{idc}\int\left(V_{DC_{set}} - V_{DC}\right).dt \quad (9)$$

$$U_{D,inv} = V_{Dg} - \left(K_{plsc}.\left(I_{Dg_{set}} - I_{Dg}\right) + K_{ilsc}\int\left(I_{Dg_{set}} - I_{Dg}\right).dt\right) - L_f\omega_e I_{Qg} \quad (10)$$

$$U_{Q,inv} = V_{Qg} - \left(K_{plsc}.\left(I_{Qg_{set}} - I_{Qg}\right) + K_{ilsc}\int\left(I_{Qg_{set}} - I_{Qg}\right).dt\right) + L_f\omega_e I_{Dg} \quad (11)$$

Here, $I_{Dg_{set}}$&$I_{Qg_{set}}$are the D and Q axis grid current set point, Q_{lsc_ref} is the reactive power set point, I_{Dg}&I_{Qg} are the D and Q axis grid current, V_{Dc}&$V_{DC_{set}}$ are the actual and set point value of DC voltage, L_f is the line filter inductance, s is the slip, ω_e is rotational speed and K_{plsc}&$K_{ilsc}$are the proportional and integral gain of the LSC converter PI controller. Once $U_{D,inv}$ and $U_{Q,inv}$ are calculated, they are converted back into three phase system and compared with triangular waves to calculate the gate signals for the LSC IGBT switches.

4. Integration of Energy Storage through DC Capacitor for providing Frequency Response

The energy storage approach to support the wind farms is not new. Different kinds of energy storage devices are already helping wind farms to provide ancillary services. Common trend is to develop the energy storage as a separate generating unit and connect it to the grid using bi-directional power electronic converter. Among the previous research work on similar approach, Sudipta Ghosh et al developed a combined system with DFIG wind turbines and energy storage device [23]. The combined system can provide inertial response and primary frequency response using the capability of the energy storage. Moreover the system can provide support in both super and sub synchronous region. Similarly Nicholas from GE in ref [24] showed that an energy storage connected separately with a wind farm can improve the performance during frequency response.

Figure 2 shows a conventional BESS system connected to the grid to support wind farm [17]. In this kind of arrangement, a battery management system is required. The battery management system keeps track of the battery and grid conditions and schedules the charging and discharging system according to that. The power converter rating depends on the total size of the battery. Control system for wind turbine is totally separated from the battery control system. It is not required to make a change to any of the controlling parameters of the wind farm and wind turbine controller.

The implementation of the described BESS integration system is simpler due to the lack of controller parameter overlapping for wind turbine and BESS. But the problem associated with the setup is, the entire energy storage power is aggregated in one place and any failure in the power converter or the BESS system affects the complete system, and it can lead to further grid faults.

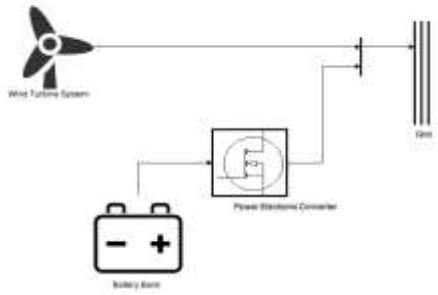

Fig. 2. BESS integrated with a wind turbine through separate converter

To move into a more distributed system, there is another approach to integrate the energy storage device at the DC capacitor of the DFIG wind turbine. The system has the major advantage that a single failure in any of the turbines will not entirely affect the whole grid system, and the chance of further fault propagation is reduced. Also it eliminates the necessity of an extra converter for the BESS. Researchers previously used this kind of setup to support the DFIG for various purposes. Liyan et al in ref [25] and Govada et al in ref [26] used super capacitor energy storage devices. Zhenhua et al in ref [27] and Aktarujjaman et al in ref [28] used battery based energy storage devices. In all these references, the energy storage is connected to the DFIG DC capacitor and the primary scope of was to reduce intermittency and improving power quality of the wind turbine output. Results available from this studies show that the combined system can produce smoother output. However those reference papers were not focused to show the improvements during the system frequency disturbance. Nicholas from GE in ref [24] and Bijaya et al in ref [29] used the BESS connected through DC capacitor of DFIG to provide frequency response support. GE showed that the combined system can vary the output power depending on the system frequency needs. The paper mentioned that the next target is to provide primary frequency response from the combined system to fulfill future grid requirements. Also the result available from ref [24] indicates that the use of energy storage eliminates the possibility of wind turbine stalling during recovery period. Bijaya et al in ref [29] showed that the combined system can maintain a steady system frequency and constant output voltage. However the results fail to demonstrate the effectiveness of providing fast frequency response.

Figure 3 shows the basic concept of the BESS interconnection in turbine level to provide frequency response used in this paper. It can be seen in the figure that the BESS is connected directly to the DC coupling capacitor. Both the DC link capacitor and the BESS use the same

power electronic converter during grid integration. A frequency sensing system is incorporated with the BESS and the power electronic converter system. Once the system senses the frequency from the grid, it compares the value with a reference value. Depending on the frequency deviation value, the operation of the BESS connected DFIG system is divided into four different regions. The regions and respective control algorithms are described below.

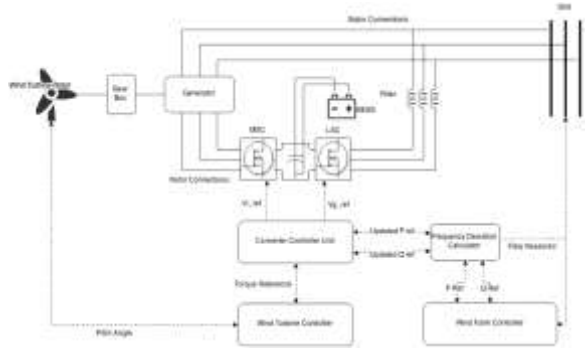

Fig. 3. BESS integrated with the DC coupling capacitor

4.1 Steady state operation

The steady-state operation indicates the time period when the grid frequency deviation remains within an allowable limit. The wind turbine operator can chose to disconnect the BESS from the dc coupling capacitor during this time period. If the BESS is disconnected, MSC and LSC current controller follows the equations (Equation 4 - 11) mentioned in the previous section for a standalone DFIG system. The wind turbine owner can also keep the BESS connected during steady-state operation. If so, the BESS helps the turbine to follow the reference values and produce smoother output power. During this study, the BESS was kept connected during steady state operation.

4.2 Discharging of BESS

Discharging of BESS is required when the grid frequency goes below the threshold of nominal value. The required extra power is supplied to the grid by the BESS. The LSC and MSC current controller algorithm and the set points require changes. Amount of frequency deviation is calculated by subtracting the actual frequency from the nominal frequency value. The frequency deviation value is then used as an input to a predefined table to identify the exact amount of extra power required to support the grid during frequency imbalance. The following equations show the BESS integrated DFIG turbine's operation during frequency deviation.

$$f_{dev} = f_{act} - f_{nom} \tag{12}$$

$$P_{ext} = table\ value\ (f_{dev}) \tag{13}$$

$$P_{tot\_req} = P_{wind} + P_{ext} \tag{14}$$

Here, f_{dev}, f_{nom}, f_{act} indicates the frequency deviation, nominal frequency value and actual measured frequency, P_{wind}, P_{ext}, and P_{tot_req} indicates the wind turbine power output, extra power required for frequency support (derived from table) and the total output power

D and Q axis current reference values for MSC control also changes. Following equations show the update in the reference value calculation

$$I_{Dr_{set}} = \frac{(P_{tot\_req} - P_{ext} - P_{lsc})}{V_{sd}} \cdot \frac{L_s}{L_m} - \frac{I_{Qs}R_s}{L_m} \tag{15}$$

$$I_{Qr_{set}} = -\frac{(Q_{ref} - Q_{lsc})}{V_{sd}} \cdot \frac{L_s}{L_m} - \left(\frac{V_{sd}}{L_m} - \frac{I_{Ds}R_s}{L_m}\right) \tag{16}$$

Here, $I_{Dr_{set}}$, $I_{Qr_{set}}$ indicates the D and Q axis rotor current set point value, I_{Ds}, I_{Qs} is the D and Q axis stator current, P_{lsc} is the LSC power, L_s, L_m are the stator side and mutual inductance and R_s is the stator resistance

Similarly the D and Q axis current reference of LSC controller also changes. Below equation shows the updated equation

$$I_{Qgset} = o \tag{17}$$

$$I_{Dg_{set}} = \frac{\sqrt{2} * P_{tot\_req}}{\sqrt{3} * V_{grid\_rms}} \tag{18}$$

Here, V_{grid_rms} is the grid voltage RMS value

The reference voltage signals are calculated using the updated current reference equations. The PWM signals for the MSC and LSC converter are then calculated by comparing the reference voltages with a highly sampled triangular signal.

4.3 Charging of BESS

Charging of BESS is required following the frequency deviation clearance. Once the frequency comes back close to the nominal value and the Battery State of Charge (SOC) goes below a certain level, the battery needs to be charged. The battery is charged in a process, where the charging current is lower than the discharging current. The charging process takes longer time than the discharging. During charging, the battery takes the current from the wind turbine itself. The wind turbine generates optimum power depending upon the wind speed. The reference power for each wind turbine in the wind farm considers the charging current for the battery and set the reference power output from the turbines according to that. D and Q axis current reference changes during charging process. The equations during the charging procedure are shown below.

$$P_{wind} = Optimum\ power\ from\ WTG \tag{19}$$

$$P_{ref} = WTG\ power\ ref.from\ the\ farm\ contr \tag{20}$$

$$I_{charge} = Battery\ charging\ current \tag{21}$$

$$P_{charge} = V_{dc} * I_{charge} \tag{22}$$

$$P_{ref\_upd} = P_{ref} - P_{charge} \tag{23}$$

Here P_{charge} is the charging power associated with the battery charging and P_{ref_upd} indicates the updated reference

power for the wind turbines. The D and Q axis current set points are calculated using the following equations

$$I_{Dr_{set}} = \frac{(P_{ref}-P_{lsc})}{V_{sd}} . \frac{L_s}{L_m} - \frac{I_{QS}R_s}{L_m} \quad (24)$$

$$I_{Qr_{set}} = -\frac{(Q_{ref}-Q_{lsc})}{V_{sd}} . \frac{L_s}{L_m} - \left(\frac{V_{sd}}{L_m} - \frac{I_{DS}R_s}{L_m}\right) \quad (25)$$

LSC current set points and the reference voltage calculation equations are given below

$$I_{Qgset} = o \quad (26)$$

$$I_{Dg_{set}} = \frac{\sqrt{2}*P_{ref\_upd}}{\sqrt{3}*V_{grid\_rms}} \quad (27)$$

4.4 Transient Period

Grid-connected wind turbines face several kinds of transient operating conditions. Wind gust, voltage dip, over voltage, low voltage ride through period are some of the examples of transient periods. Depending on the transient condition identified, the wind farm controller calculates the required active and reactive power set points for the wind turbines. The turbines use the reference values to calculate the D and Q axis current set point for the MSC and LSC controller. The complete analysis of the transient periods is out of scope of this paper.

4.5 Battery System Sizing to Provide Required Support

It is important to calculate proper size of the BESS to provide required amount of power support during emergency. BESS system consists of several series and parallel connected battery cells. The series connected battery cells ensure the right amount of voltage output from the BESS. The parallel connected battery cells ensure the current output from the BESS. Proper sizing of the BESS depends on several other parameters such as DC link voltage (V_{dc}), Median voltage of the battery cell (V_{med}), Wind turbine power (P_{turb}), Support level from battery ($n_{support}$), Depth of Discharge (DOD), Cell capacity ($I_{cell\ cap}$) and C rate used during charging or discharging (C_r).

Proper sizing of the BESS also depends critically on the value of the maximum power it needs to provide during emergency condition and the minimum duration it needs to provide the support. These two values are often defined by the system operator where the wind farm is located. As an example Ontario Independent System operator requires the wind turbine to increase 10% of available output for at least 10seconds during emergency condition [30].

Considering the BESS needs to provide a maximum of $n_{support}$% of the turbine nominal power for $T_{support}$ seconds during emergency condition

$$P_{BESS} = \frac{P_{turb}*n_{support}}{100} \quad (28)$$

As, the BESS produces DC power output,

$$P_{BESS} = V_{BESS} * I_{BESS} \quad (29)$$

To integrate the BESS with DC link capacitor it is essential that the DC link voltage matches closely with the BESS voltage ($V_{BESS} = V_{dc}$).

As previously mentioned, that the aggregated BESS voltage is achieved by series connecting a number of single battery cells. If the median voltage rating of a single battery cell is V_{med}, then the total number of series connected battery cells to produce the V_{BESS} are

$$n_s = \frac{V_{dc}}{V_{med}} \quad (30)$$

Similarly the current I_{BESS} is generated by connecting a number of battery packs in parallel (n_p).In each pack,n_s numbers of series connected single battery cells are required. The single battery cell output current during discharging depends on the cell capacity ($I_{cellcap}$) and the C rate used. The C rate defines the rate of discharge of the battery cell. For high C rate, the battery cell produces high output current, but discharge quickly and also has an overall adverse effect on the life cycle of the battery life. For a battery cell capacity of $I_{cellcap}$ and C rate of C_r, the number of parallel battery packs required are

$$n_p = \frac{I_{BESS}}{I_{cellcap}*C_r} \quad (31)$$

Combining equation 28, 29, 30 and 31

$$n_p = \frac{P_{turb}*n_{support}}{100*V_{dc}*I_{cellcap}*C_r} \quad (32)$$

The time duration measure (in minutes) to determine how long the BESS will support the grid is dependent on the C rate and depth of discharge. Depth of Discharge (DOD) is the difference between the starting and ending SOC of the battery during operation. Theoretically battery SOC changes from 100% to 0 % in 1 hour if the battery discharges at the rated current($C_r = 1$). The relation between C rate and discharge time for a battery to move from SCR 100% to 0% is inversely proportional. If a depth of discharge level of DOD and a C rate of C_r is used during battery operation, then battery support time (in minutes) will be decided by the following equation

$$T_{support} = \frac{DOD*60}{100*C_r} \quad (33)$$

The IGBT, grid connection cable and the transformer rating needs to be increased to handle the extra power coming through the BESS. IGBT voltage rating remains same, but the current rating needs to be increased to sustain turbine and BESS current (I_{turb}+I_{BESS}). Grid connection cable and transformer's rating needs to be increased to handle the turbine and the BESS power (P_{turb}+P_{BESS}).

Actual configuration of the series and parallel connected stacks can be modified depending on where the BESS is installed and the available space. Depending on the actual nacelle configuration and accessories, the BESS can be installed either in the nacelle or down tower. It is recommended, to install the BESS at down tower. It has the advantage of easy access during maintenance and also a temperature control unit can be installed. This will improve

the overall BESS lifespan. Also it ensures the nacelle experiences less weight and stress.

If the BESS is installed down tower, then it is important to consider the voltage drop and power loss through the DC cable during Battery sizing calculation. Considering the BESS drop is V_{drop} and power loss is P_{drop} due to the DC connecting cable between the BESS and DC capacitor voltage, then equation 30 and 32 needs to be updated accordingly

$$n_s = \frac{V_{dc}+V_{drop}}{V_{med}} \quad (34)$$

$$n_p = \frac{\left(P_{turb*}{}^{n_{support}}/_{100}\right)+P_{drop}}{V_{dc}*I_{cellcap}*Cr} \quad (35)$$

4.6 Control Flowchart of the Battery

Control logic for all four periods stated before, works by inspecting the SOC condition of the battery. It is critical to identify the SOC range the battery will be operating. Battery voltage vs. SOC and battery degradation over the depth of discharge is the two parameters need to be considered during the SOC range selection and control algorithm development. During the study, the battery voltage vs. SOC is plotted using the generic Li-Ion battery model available in the Matlab/Simulink library. Figure 4 shows the Li-Ion voltage vs. SOC during charging. From the figure it is evident that the battery voltage remains fairly linear during the range of 30% to 80% SOC. As a conservative approach, the SOC limit from 40% to 80% is selected for operation during this study.

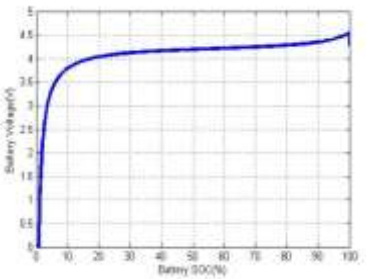

Fig. 4. Battery voltages vs. SOC of a single Li-Ion battery cell

This selection helped to ensure two things. First, it ensures that the battery operating voltage remains linear during operation. This helps to integrate the battery with the DC link and control the DC voltage properly. Second, it ensures relatively lower depth of discharge (40%). Lower depth of discharge increases the overall battery life. The maximum and minimum SOC limit and the depth of discharge can be varied depending on the battery technology and by analyzing the battery characteristics.

The charging and discharging action is triggered based on the system frequency and the SOC level. During the normal system condition (frequency remains within threshold limit), the battery starts charging if the SOC level reaches below 60%. This ensures that the battery does not drain itself too much and the battery connected wind turbine system keeps enough reserve for the emergency situation. As soon the battery system reaches the maximum SOC level (80%), the battery stops charging. Considering the power system remains in normal condition, the battery can help the wind turbine to follow power set points and produce smooth outputs. As soon as the system experiences major power imbalance, the control algorithm enters into emergency mode and detects whether the actual system frequency violated the threshold values in positive (system frequency above 60Hz+threshold) or negative direction (system frequency below 60Hz-threshold). If the system frequency violates the frequency threshold in positive direction, the battery keeps charging till the maximum SOC limit (80%). If the frequency deviation clears before it reaches 80% SOC then the control algorithm enters the normal operation, but if the system frequency deviation remains and the battery SOC reach the maximum value, then battery disconnects and connects again once the frequency deviation is cleared. Similarly if the system frequency violates the frequency threshold in negative direction, the battery keeps discharging till the minimum SOC limit (40%). If the frequency deviation clears before it reaches 40% SOC then the control algorithm enters the normal operation mode. But if the system frequency deviation remains and the battery SOC reach the minimum value, then battery disconnects. It connects again and starts charging once the frequency deviation is cleared. Figure 5 shows flowchart of the control logic.

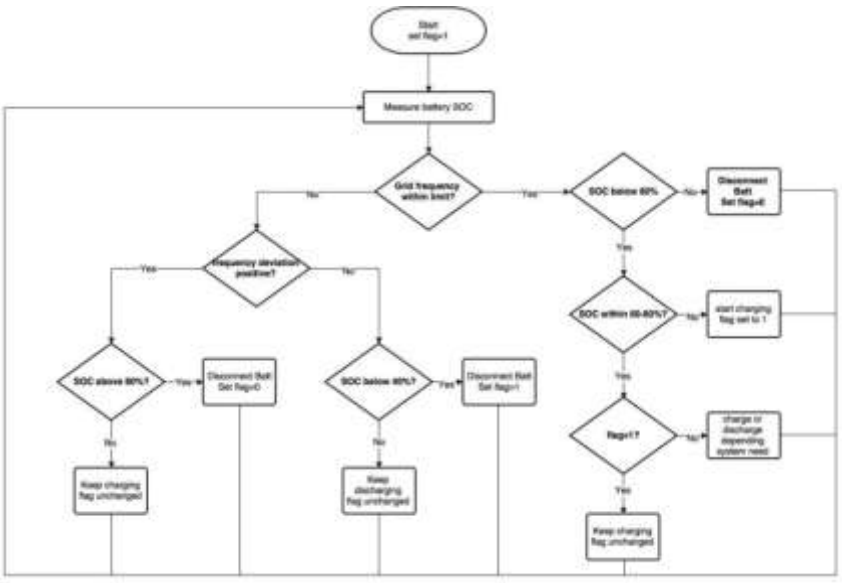

Fig.5. Energy storage control flow chart

5. Simulation & Results

A simple two area power system network was developed in MatLab/Simulink to simulate the frequency deviation incident. Figure 6 shows the one-line diagram of the developed system. There are five synchronous generators, each with a capacity of 1 MW. There is a load (load 1) in the system which is matching with the total generated power in the system. There is a power imbalance created by switching on another load (load 2). The load creates a power imbalance of 20%.

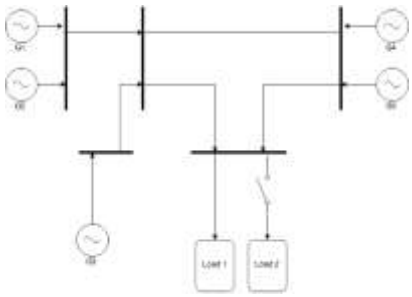

Fig. 6. Two area power system network with five synchronous generator

During the simulations, focus was kept on initial stages of frequency response, especially the reduced inertial response due to integration of wind turbines and how the introduction of energy storage helps. Synchronous generator governor droop, secondary frequency control and AGC method is already well developed in the industry and not discussed in detail in this study. Moreover, secondary frequency response and Area Generation Control (AGC) was not implemented in the simulations.

The system was initially simulated to see the frequency deviation and inertial response by the synchronous generators during power imbalance. The system was running in balanced condition. At 25 seconds, using load 2, a power imbalance of 20% is created. The result is shown in figure 7(a). Figure 7(b) indicates the frequency drops significantly from the nominal value.

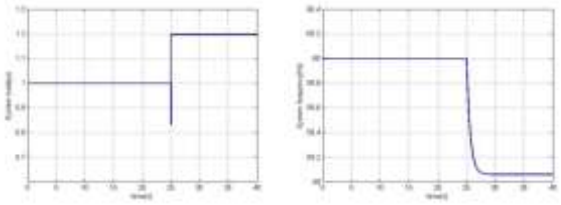

(a) (b)

Fig. 7(a). System Load increase due to switch in extra load; **(b).**Frequency deviation due to Power Imbalance

Synchronous generators respond to the frequency deviation by slowing down and increasing the output power through the release of stored kinetic energy. The increased power output is shown in figure 8.

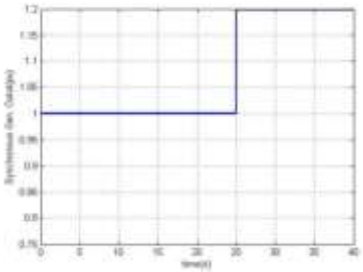

Fig. 8. Release of kinetic energy from synchronous generators during frequency deviation

Generally in a synchronous generator, the inertia constant varies between 2-8 s. The system with 20% power imbalance is simulated by varying the synchronous generators inertia constant from 2-8 s. Figure 9 shows the results.

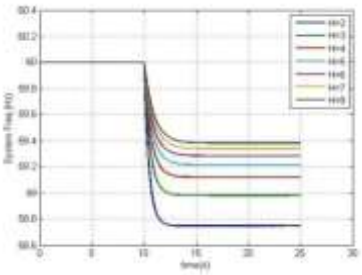

Fig. 9. Variation of minimum frequency value and ROCOF with different system inertia level during power imbalance

From the figure it can be visible that, for higher inertia constant, the frequency deviation and ROCOF are lower.

As stated previously, wind turbines normally don't add any inertia to the system. To inspect the effects of connecting wind turbines in the system and variation in frequency response, one of the synchronous generators is replaced with a DFIG wind turbine. For the simulation purpose, built in DFIG wind turbine model available in MatLab/ Simulink is used. Figure 10 shows the system single line diagram with wind turbine integrated.

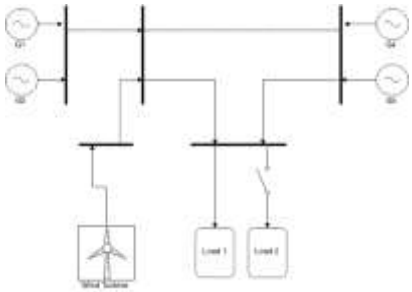

Fig. 10. Wind integrated a two-area power system

Again a power imbalance is created at 25 second. The result in figure 11 indicates that the wind turbine did not increase power during frequency imbalance. It only creates a small oscillation in the output power due to the transient load condition.

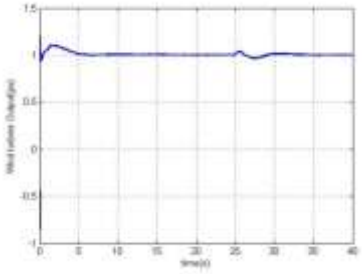

Fig. 11. Wind Turbine output without BESS support during frequency deviation

Next, the wind energy penetration is varied between 10-30% of total generated power. The frequency deviation is observed during a power imbalance of 20%. Figure 12 shows the results.

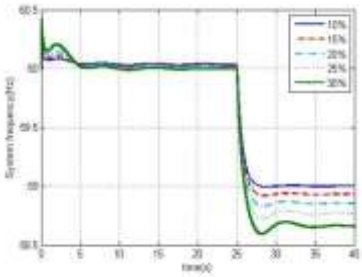

Fig. 12. Frequency deviations with different wind energy penetration level

From the figure it is obvious that higher penetration of wind energy in the grid is reducing system inertial response and also increasing frequency deviation. Table 1 indicates the detailed result of the analysis with different wind penetration level.

Table 1. Frequency deviation with different wind energy penetration

Wind Penetration(%)	F nadir	F Settling	Deviation(%)
10	58.99	59.00	1.66
15	58.91	58.93	1.78
20	58.82	58.85	1.91
25	58.72	58.76	2.06
30	58.58	58.65	2.24

Next, the BESS is connected to the wind turbine through the DC capacitor. Figure 13 shows the BESS connected wind turbine system.

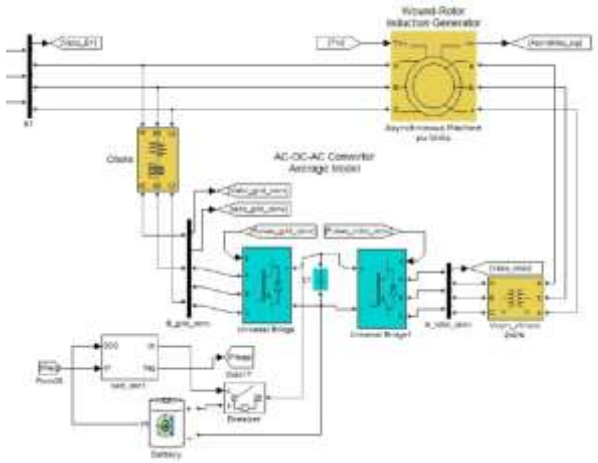

Fig. 13. BESS connected through the Wind Turbine DC Capacitor

Figure 13 shows the DFIG stator side is connected directly to the grid, rotor side is connected through the AC/DC/AC converter. BESS is connected with the DC Capacitor. The battery model shown in the figure is Matlab built-in generic battery model. The breaker is operated by sensing the Battery SOC condition and the frequency

deviation. If SOC is more than 80% or less than 40%, the breaker opens to disconnect battery.

The BESS is sized to provide 20% support of the wind-turbine power output. The case is simulated considering there is 20% of wind penetration. During simulation, 20% power imbalance is created by varying the interruptible load. Figure 14 shows the output of the BESS coupled wind turbine. The results confirm that during the power imbalance incident, along with the synchronous generator, the BESS connected wind turbine also increases its output to stabilize the grid. The extra power is supplied by the BESS.

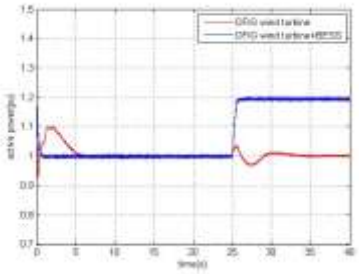

Fig. 14. Power increase of BESS connected WT during frequency Deviation

Figure 15 shows the SOC condition of the battery. During the initial period, the BESS SOC remains close to the initial value, But at 25s when the power imbalance occurs, the battery starts discharging and the SOC reduces.

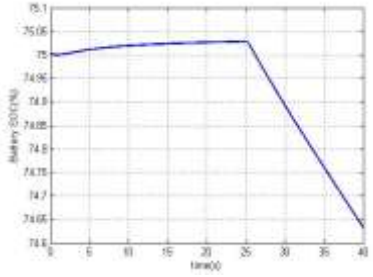

Fig. 15. SOC condition of the Battery during providing the frequency response

The battery is capable of providing 20% support of nominal wind turbine power output even when the available wind power is low. Such case is simulated and shown in figure 16. Available wind power from the wind speed was 0.28pu of the nominal value. Frequency deviation occurs at 25 s and the battery was able to provide full 20% support of the nominal wind turbine power to help stabilizing the system. The total output raises to 0.48pu from the battery connected DFIG.

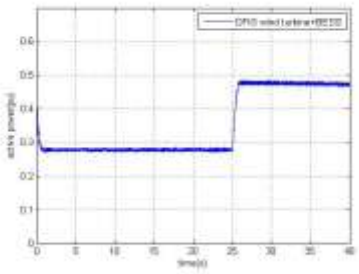

Fig. 16. BESS Support during low wind turbine output

Figure 17 shows the performance of the system with and without BESS is connected with the wind turbine. The blue signal shows the response without BESS connected and red signal shows the response with BESS connected. From the figure, it is obvious that the BESS connected wind turbines significantly reduces the frequency nadir during power imbalance.

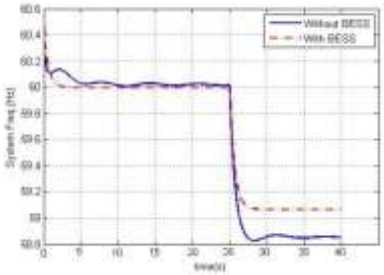

Fig. 17. Frequency Deviation with and without BESS integrated

Figure 18 shows the battery current during charging and discharging incident. Initially, there was a power imbalance within the system and the battery was providing support to the grid by discharging current. At 25 seconds, the fault is cleared and BESS starts charging by taking current from the wind turbine. Figure 18 shows the BESS connected wind turbine power output and Figure 19 shows the SOC variation during the process.

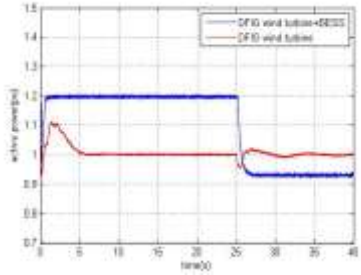

Fig. 18. Wind Turbine Power output during discharging-charging incident

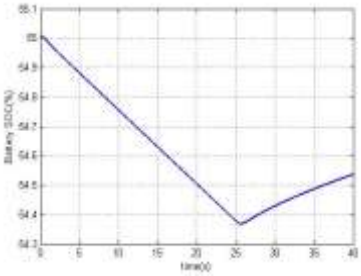

Fig.19. Battery SOC during discharging-charging incident

The discharging current C rate is twice of the charging current, thus charging process takes more time than the discharging. The governor set point for the synchronous generators can be set at a higher value or the reserve generating unit outputs are set accordingly to offset the

reduced power output from the BESS connected wind turbine.

A comparison between the system response is done when BESS is connected through the DC capacitor and when the BESS is connected through a separate converter system. The results are shown in figure 20.

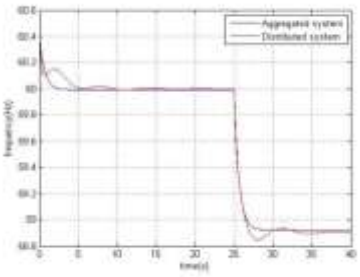

Fig.20. System responses while BESS is connected through DC Capacitor & through a separate converter system

In the figure 20, red line shows the system response while the BESS is connected through a separate converter, and blue line shows the response when BESS is connected through the DC capacitor. Results indicate that if similar size of battery is used, the system response performance is similar for both cases. However, there is oscillation visible when the BESS is connected through a separate system. Also the frequency drops to a lower value in this case during the transient period. For the other case, when the BESS is connected through the DC capacitor, it produces a smoother frequency response. There is also a possibility of higher harmonic injection when the BESS is connected through a separate converter system. Operation of the IGBT switches in the extra converter used for BESS integration increases the harmonic injection. Harmonic injection for both system configurations are calculated until 50th order and shown in figure 21.

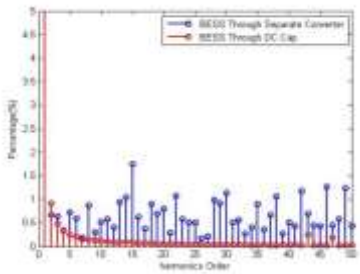

Fig. 21. Harmonic Performance in different BESS integration method

Total harmonic distortion value for the system is 3.10%when BESS is connected through the separate converter. BESS connected through the DC capacitor produces better result by injecting low Total harmonic distortion of 1.23%.

The results indicate that energy storage connected through the DC cap provides better performance in terms of harmonics injection to the grid. The method can provide the required level of support and improve the system frequency response along with providing smooth output and lower harmonic injection.

6. Conclusion

The paper demonstrated that integration of the energy storage effectively enables the type 3 wind turbines to increase its power output and improve the frequency response during the times of power imbalance. Frequency response through energy storage integration is better as it provides faster response and removes the danger of wind turbine stall. It is also shown in the paper that the system performs better when the energy storage is connected through the DC cap of the type 3 wind turbine. This method of energy storage connection requires minimal changes to the hardware of the wind-turbine and mainly focuses upon the adjustment in the control algorithm. The adjusted control shown in this paper successfully operates the energy storage charging and discharging while connected to the DFIG wind turbine capacitor. The method is validated by the results available from the simulation. The wind-turbine converter controller operates the energy storage device. So there is no necessity of a separate battery controller device. Energy storages connected through the wind turbine DC cap provides the frequency response solution in a distributive manner, which provides robust support. If one or more turbines fail, other turbines in the farm can still provide the frequency response. It helps to bring back the system stability. Finally, it is reviewed in this paper that proper integration of energy storage with the DFIG wind turbine can improve frequency response issues. With further study and analysis, a similar approach can be adopted for other renewable energy sources such as solar.

Reference

[1] 20% Wind Energy by 2030; Increasing Wind Energy's Contribution to U.S. Electricity Supply, U.S. Department of Energy, 2008.
[2] Robert W. Cummins, NERC Frequency Response Initiative, National Renewable Energy Laboratory, January 27, 2011.
[3] NERC, Frequency Response Standard Whitepaper, April 6, 2004.
[4] Emmanouil Loukarakis, Ioannis Margaris and Panayiotis Moutis, "Frequency Control Support and Participation Methods Provided by Wind Generation", IEEE Power and Energy Conference, 2009
[5] E. Muljadi, V. Gevorgian, M. Singh and S. Santoso, "Understanding Inertia and Frequency Response of Wind Power Plants", Presented at the 2012 IEEE Symposium on Power Electronics and Machines for Wind Applications (PEMWA 2012)on July 16-18, 2012 in Denver, Colorado
[6] Zhinxin Miao, Lingling Fan, Dale Osborn and Subbaraya Yuvarajan, "Wind Farms with HVDC Delivery in Inertial Response and Primary Frequency Control", IEEE transaction on Energy Conversion, Vol. 25, No. 4, December 2010

[7] N. R. Ullah, T. Thiringer, and D. Karlsson, "Temporary Primary Frequency Control Support by Variable Speed Wind Turbines – Potential and Applications", IEEE Trans. Power Systems, vol. 23, no. 2, pp. 601-612,May 2008
[8] M. Kayikci and J. V. Milanovic, "Dynamic Contribution of DFIG-based Wind Plants to System Frequency Disturbances", IEEE Trans. Power Systems,vol. 24, no. 2, pp. 859-867, May 2009
[9] J. Morren, J. Pierik and S. W.H. de Haan, "Inertial Response of Variable Wind Turbines", Electric Power Systems Research,Elsevier, pp. 980-987,Wind Energy, vol. 76, 2006.
[10] D. Margaris, A. D. Hansen, P. Sorensen and N. D. Hatziargyriou, "Investigating Power Control in Autonomous Power Systems with Increasing Wind Power Penetration", Presented in 8th InternationalWorkshop on Large-Scale Integration of Wind Power into PowerSystems as well as on Transmission Networks for Offshore Wind Farms, 14-15 Oct. 2009, Bremen, Germany.
[11] P. Tielens and D. Van Hertem, "Grid inertia and frequency control in power systems with high penetration of renewables", Young Researchers Symposium in Electrical Power Engineering, Delft, vol. 6, April 2012.
[12] N. A. Jansens, G. Lambin, and N. Bragard, "Active Power Control Strategies of DFIG Wind Turbines", IEEE PowerTech, Lausanne, Switzerland, July 2007
[13] K. V. Vidyanandan and Nilanjan Senroy, "Primary Frequency Regulation by Deloaded Wind Turbines Using Variable Droop", IEEE transactions on Power Systems, Volume 28, Issue 2, May 2013
[14] Gowaid, A. El-Zawawi, and M. El-Gammal, "Improved Inertia and Frequency Support from Grid-Connected DFIG Wind Farms",IEEE/PES Power Systems Conf. and Expo. Phoenix, AZ, USA, Mar. 2011
[15] Maria A. Henley, National Energy Technology Laboratory, Frequency Instability Problems in North American Interconnections, May 1, 2011
[16] Antony Johnson, National Grid, Grid Code Frequency Response Working Group System Inertia, Available: http://www.nationalgrid.com/NR/rdonlyres/4852C28A-5D61-4755-B50A-38E5DD3C9D3F/39861/SimuatedInertia_090210.pdf. Accessed: 07/18/2014
[17] Sercan Teleke, PhD dissertation, Control Methods for Energy Storage for Dispatching Intermittent Renewable Energy Sources, North Carolina State University, 2009
[18] P. F. Ribeiro, B. K. Johnson, M. L. Crow A. Arsoy, and Y. L. Liu, "Energy Storage Systems for Advanced Power Application", IEEE, vol. 89, no. 12, pp. 1744–1756; Dec. 2001
[19] J. McDowall, "Conventional Battery Technologies—Present and Future", IEEE Power Engineering Society Summer Meeting, vol. 3, pp. 1538–1540, July 2000
[20] B. Roberts, "Capturing Grid Power", IEEE Power and Energy Mag., vol. 7, no. 4, pp. 32 - 41, July-Aug. 2009.
[21] Nickel- metal hydride battery. Available: http://en.wikipedia.org/wiki/Nickel%E2%80%93metal_hydride_battery. Accessed: 07/18/2014
[22] Sandeep Nimmagadda, PhD Dissertation, Advanced Solutions to the Grid Interconnection Issues due to Large Scale Integration of Wind Energy,Texas Tech University; June 2014
[23] Ghosh, Sudipta, Sukumar Kamalasadan, Nilanjan Senroy, and Johan Enslin. "Doubly fed induction generator (DFIG)-based wind farm control framework for primary frequency and inertial response application.", IEEE Transactions on Power Systems, vol. 31, no. 3, pp. 1861-1871, May 2016
[24] Nicholas W. Miller, GE energy, GE experience with Turbine Integrated Battery Energy Storage, Available: http://www.ieee-pes.org/presentations/gm2014/PESGM2014P-000717.pdf, Accessed: 07/30/2016
[25] Qu, Liyan, and Wei Qiao. "Constant power control of DFIG wind turbines with supercapacitor energy storage." IEEE Transactions on Industry Applications, vol. 47, no. 1, pp. 359-367, Nov. 2010
[26] Ganesh, Govada Panduranga, and Arjuna Rao. "Super-Capacitor Energy Storage of DFIG Wind Turbines with Fuzzy Controller.", International journal of Engineering Research and Development, vol. 10, no. 12, pp. 52-66, December 2014
[27] Jiang, Zhenhua, and Xunwei Yu. "Modeling and control of an integrated wind power generation and energy storage system." 2009 IEEE Power & Energy Society General Meeting, pp. 1-8. IEEE, 2009.
[28] Aktarujjaman, M. D., Mohammad A. Kashem, Michael Negnevitsky, and Gerard F. Ledwich. "Smoothing output power of a doubly fed wind turbine with an energy storage system.", In Proceedings Australian Universities Power Engineering Conference, 2006
[29] Bijaya Pokharel, Olorunfemi ojo and Adeola Balogun, “Standalone operation of a DFIG-based wind turbine system with integrated energy storage”, International Symposium on Power Electronics fir Distributed Generation Systems (PEDG), pp. 1-5, June 2015
[30] Ontario Independent Electricity System Operator, LRP I RFP Backgrounder - Connection, Available: http://www.ieso.ca/Documents/generation-procurement/lrp/lrp-1-final/LRP-I-RFP-Backgrounder-Connection.pdf, Accessed: 04/10/2016